



HAL
open science

Correlation between Structural Parameters and Property of PE Blown Films

Shokoh Fatahi, Abdellah Ajji, Pierre G. Lafleur

► **To cite this version:**

Shokoh Fatahi, Abdellah Ajji, Pierre G. Lafleur. Correlation between Structural Parameters and Property of PE Blown Films. *Journal of Plastic Film and Sheeting*, 2005, 21 (4), pp.281-305. 10.1177/8756087905059979 . hal-00572066

HAL Id: hal-00572066

<https://hal.science/hal-00572066>

Submitted on 1 Mar 2011

HAL is a multi-disciplinary open access archive for the deposit and dissemination of scientific research documents, whether they are published or not. The documents may come from teaching and research institutions in France or abroad, or from public or private research centers.

L'archive ouverte pluridisciplinaire **HAL**, est destinée au dépôt et à la diffusion de documents scientifiques de niveau recherche, publiés ou non, émanant des établissements d'enseignement et de recherche français ou étrangers, des laboratoires publics ou privés.

CORRELATION BETWEEN STRUCTURAL PARAMETERS AND PROPERTY OF PE BLOWN FILMS*

Shokoh Fatahi,^{1,†} Abdellah Aji² and Pierre G. Lafleur¹

¹*École Polytechnique de Montréal, Chemical Engineering Department
CRASP, CP 6079, Succ. Centre-ville, Montréal, Québec, H3C 3A7 Canada*

²*Industrial Materials Institute, NRC, 75 Boul. De Mortagne
Boucherville, Québec, QC, J4B 6Y4 Canada*

ABSTRACT: Our objective in this study is to develop models which relate detailed structural parameters to performance, providing the means for predicting final film properties. In this work, we used different types of polyethylene (LLDPE, HDPE, and LDPE) at different process conditions in the film blowing process. The morphology of films was studied using X-ray diffraction, SEM, AFM, FTIR, and birefringence measurements. Herman's orientation factors of the films were determined via both WAXD pole figures and infrared dichroism. DSC, WAXD and SAXS were used to determine microstructural parameters including the degree of crystallinity, lamellar thickness, crystal size, length of crystal, and long spacing. By using the statistical design of experiments, a correlation between mechanical properties including tensile properties, Elmendorf tear, dart impact, and optical properties such as haze and clarity was obtained with the microstructural parameters.

KEY WORDS: microstructure, mechanical properties, optical properties, physical properties, blown films, LLDPE, LDPE, HDPE, crystallinity, morphology, modeling, effects of processing variables.

*This article was originally presented at the Polymer Films and Fibers 2004 Symposium of the National Research Council of Canada, which was held in Boucherville, Quebec, Canada in September 2004.

†Author to whom correspondence should be addressed. E-mail: shokoh.fatahi@polymtl.ca
Figures 3–11 appear in color online: <http://jpf.sagepub.com>

INTRODUCTION

POLYETHYLENE (PE) BLOWN film is one of the most important polymeric products today. Because of the commercial significance of PE in blown film applications, PE film manufacturers have been aggressive in improving film properties and reducing manufacturing cost to become more competitive in the global market. It is known that in the film blowing process, the primary molecular parameters are coupled with processing conditions to produce the final film morphology, which in turn determines the final film properties. In addition to these primary molecular parameters, the molecular orientation imparted during blown film is known to have a major effect on the mechanical properties of films. Therefore, characterization of film morphology is crucial for finding the structure and property relationships.

Process variables in the blown film process include:

- Temperature of the melt leaving the die
- Die gap
- Blow up ratio (BUR), defined as the ratio of final film-tube diameter to die diameter
- Take up ratio (TUR), defined as the ratio of film velocity at the nip roll to average velocity of film leaving the die
- Frost line height and cooling conditions

Figure 1 shows the schematic of the effects of molecular structure and processing induced secondary film structure (morphology and molecular orientation) on the mechanical properties of PE blown films.

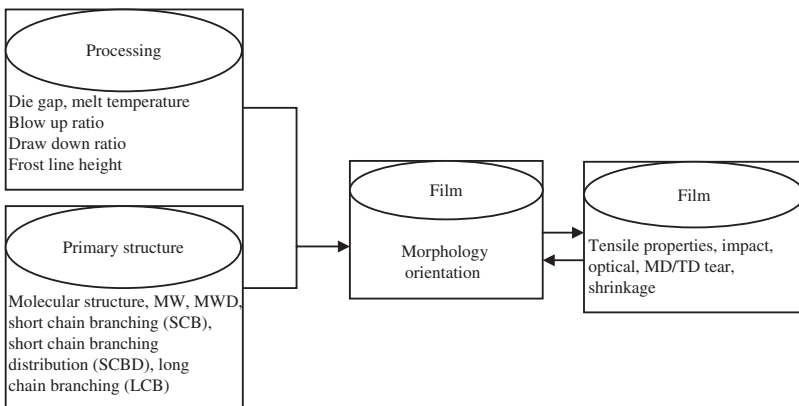


Figure 1. Schematic of effects of the structure and processing conditions on the mechanical properties.

Since the same polymer run at different conditions on the same equipment result in a variation of film properties and optical properties, changes in the blown film process parameters, including cooling which influences frost line height, have an impact on final film properties. Physical and mechanical properties of polyethylene are known to be strongly influenced by morphology, such as molecular orientation, size, shape, and characteristics of crystalline domains. Therefore fundamental structure–property (S-P) relationships in PE blown films are important to blown-film manufacturers. Understanding of the S-P relationships should enable film manufacturers to predict the physical and mechanical properties of films and to determine the processing conditions or resin properties required for achieving certain film properties.

A number of studies have been reported in recent years concerning the interrelations among processing, film structure, and physical properties of the films – and it has been well-recognized that the properties of blown films are greatly influenced by structure development during their fabrication. But from the various literature studied on this subject, it seemed that this field lacked the full development of relating the molecular structure to the properties of blown films. Therefore, it was decided to start this work aimed at a fundamental understanding of the structure–property relationships in polyethylene blown films with a goal to establish a model for predicting final film properties of different types of polyethylene (LLDPE, HDPE, LDPE) in the film blowing process [1–16].

EXPERIMENTAL

Materials

HDPE, LDPE, and LLDPE were investigated. These materials were provided by Dow Plastics Company and Nova with the specifications listed in Table 1.

Table 1. Specification of materials.

Grade	MFI (g/10 min)	Density (g/cm ³)	Mw	Mw/Mn	Manufacturer
LDPE 503A	1.9	0.923	80,900	5.02	Dow Plastics Company
LDPE-Octene FP 120-A	1	0.92	103,200	3.38	Nova Company
HD58A	0.41	0.957	193,885	12.94	Dow Plastics Company

Film Preparation

PE blown films with different structures were produced at two locations. A 45 mm diameter Killion single screw extruder with a helical annular die (outer diameter of 63.5 mm and a gap of 3 mm), a dual lip air ring with air cooling and take up equipment was used in the École Polytechnique de Montreal for all the HDPE and LDPE samples. The mass flow rate was maintained around 2.5 kg/h by adjusting the screw speed. For the LLDPE samples, we used a Brampton Engineering blown film extrusion line (die diameter of 101.6 mm and die gap of 1.1 mm) equipped with air cooling and using five extruders at the Industrial Materials Institute (IMI) of the National Research Council of Canada in Boucherville, Quebec. A mass flow rate of around 20 kg/h was maintained by adjusting the screw speeds of the five extruders which were maintained at the same temperature.

The process conditions for these films are summarized in Table 2. The preparation of films with different structures was based on changing the process conditions, particularly varying the take up ratio (TUR) and the blow up ratio (BUR) for each type of polyethylene, while maintaining a stable bubble.

Morphological Observations

Scanning Electron Microscopy

Molecular orientation and structure development during film blowing have a major effect on mechanical and physical properties of polyethylene films; therefore comprehensive and detailed morphological characterization of PE blown films was the core work. The film samples were observed using field emission gun-scanning electron microscopy (FEG-SEM). As an example, the SEM images for one sample of each different type of polyethylene films (LLDPE, LDPE, and HDPE) are shown in Figure 2. The PE film specimens were etched by soaking for 20 min in a 0.7% solution of potassium permanganate in a mixture of 65% vol sulfuric acid and 35% vol orthophosphoric acid.

Atomic Force Microscopy

The surface morphologies of films were evaluated using Digital Instrument Nanoscope IV Scanning Probe Microscope operated in multimode (Veeco Metrology Group). It was used for quick determination of surface roughness of the film and to find the images of the

Table 2. Process condition for selected samples.

	LDPE0	LDPE3	LDPE5	LDPE7	LDPE10	LDPE11	LDPE12	LDPE13	HDPE2	HDPE5	HDPE8
TUR	30.5	20	30.5	42	42	52.5	42	64	42	64	107.5
BUR	1.7	1.92	1.5	1.29	1.47	1.6	1.64	1.5	1.05	0.88	0.9
FLH (in)	7.5	9	6	5	9	7	5	6	5.5	5.5	7
	HDPE1n	HDPE2n	HDPE4n	HDPE6n	HDPE7n	HDPE9n	HDPE10n	LLDPE1	LLDPE5	LLDPE9	LLDPE10
TUR	30.5	42	64	85.5	96.5	107.5	107.5	22	15	22	30
BUR	1.35	1.15	1.25	1	1.08	0.88	0.82	2.1	3	2.1	1.5
FLH (in)	6	6	6	6	6	6.5	6.5	10	12	17.2	10

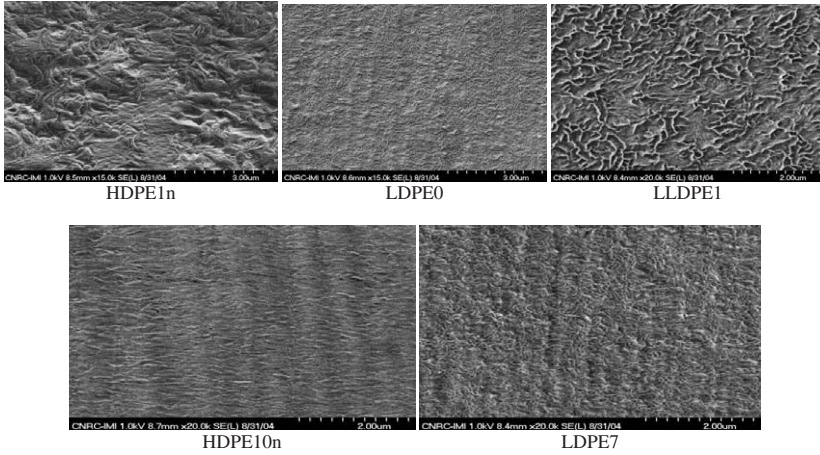


Figure 2. SEM images of blown PE films (Machine Direction ↑, Transverse Direction →).

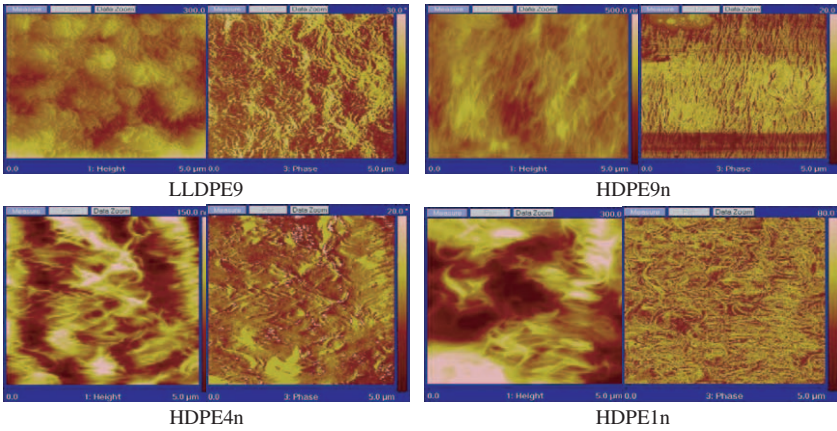


Figure 3. AFM images of the surfaces of blown films.

different structures in the various blown films. Tapping modes of AFM were used to observe surface morphology (topography) of the films at room temperature. The AFM images can accumulate three types of images such as height and phase and amplitude types. In the phase images, brighter regions represent the hard crystalline phase and the darker regions usually represent the soft amorphous phase.

Typical surface images and 3D images are shown in the Figures 3 and 4 for LDPE, LLDPE, and HDPE. The surface roughness

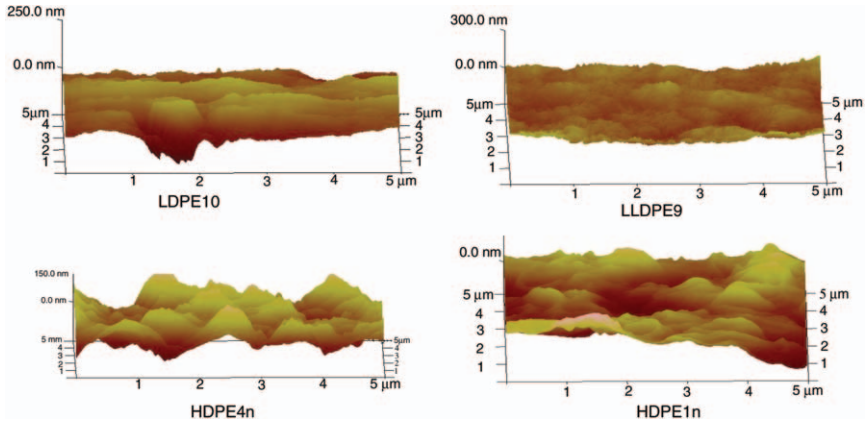


Figure 4. 3D surface plot analysis of AFM height images of blown films.

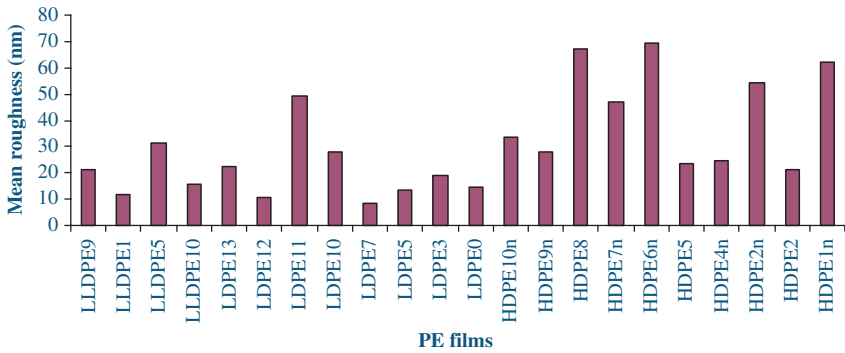


Figure 5. The surface roughness of the samples measured by AFM.

of the samples was determined by AFM and is shown in Figure 5. The surface roughness of the HDPE films was generally higher than LDPE and LLDPE.

Wide-angle X-ray Diffraction (WAXD)

WAXD is a useful technique for understanding oriented semi-crystalline polymers, and it was used for the determination of the crystal size and crystal orientation. The use of wide-angle X-ray pole figures allows one to obtain considerable information regarding the orientation of specific crystalline axes or planes. The average size

of the crystalline regions (P) was determined by using the Scherrer formula [9]:

$$P = \frac{0.89\lambda}{\beta \cos \Theta_{110}} \quad (1)$$

where β is the full width at half maximum, Θ is the Bragg's angle, and λ is the wavelength.

The transverse dimension of crystallites is calculated by:

$$L_t = \frac{0.94\lambda}{\beta \cos \Theta_{200}} \quad (2)$$

The crystalline mass fraction or degree of crystallinity is obtained through:

$$X_{C \text{ mass}} = \frac{A_c}{A_a + A_c} \quad (3)$$

A_a = area under amorphous hump and A_c = area remaining under the crystalline peaks.

The WAXD experiments were performed using a Bruker D8 Discover apparatus. The instrument with a Cu- K_α radiation (wavelength of 1.54 Å) was operated at 40 kV and 40 mA. From the WAXD pole figure technique (the (110) and (200) reflections were used), the orientation parameters, the degree of crystallinity (X_c), and the average crystallite size in (200) and (110) were determined. WAXD pole figure technique was used to obtain quantitative information about crystal orientation.

Small Angle X-ray Scattering (SAXS)

SAXS is an effective tool for studying the crystalline structure in polymers at angles very close to the main beam, typically $<2^\circ$. SAXS measures the distance between PE crystal centers, which is in the range of hundreds of angstrom units. Most frequently, the only cooperative reflections that usually appear in the SAXS patterns occur as a consequence of the periodic arrangement of crystal lamellae along the chain-axes (c-axis) direction. This is because there is considerable disorder in crystal matching in the other two directions from crystallite to crystallite. Since the Long spacing measures the distance between crystal centers, it includes the non-crystalline phase between the

crystals in the *c*-axis direction as well. In fact, the intensity of the SAXS is inversely proportional to the square of the electron density difference between the crystalline and non-crystalline regions.

The SAXS intensity distribution curves for different PE samples are shown in Figure 6. SAXS was carried out to determine Long spacing (L), the length of the crystallites and the average length of the amorphous layer. The well-known Bragg relation is used:

$$s = \frac{2 \sin \Theta}{\lambda} \quad (4)$$

$$\lambda = 1.54 \text{ \AA}$$

where λ is the wavelength and s is the scattering vector. Direct application of Bragg's law to the maximum of the scattering curve (Figure 6) yields the long spacing $L = 1/s$ (at maximum point of scattering curve), where L is the average length of the crystalline layer plus the amorphous layer. The average crystal length follows from the knowledge of L and percentage crystallinity of the polymer, typically:

$$\text{Crystal length} = L \times \text{Volume fraction crystallinity} \quad (5)$$

SAXS results indicate that the samples crystallized with a stacked lamellar morphology, with the lamellar normals oriented parallel to MD. The existence of the randomly oriented lamellae has been seen in the LDPE and LLDPE samples.

Infrared Dichroism using FTIR Spectroscopy

Infrared dichroism obtained from polarized FTIR spectroscopy is a technique for the determination of crystalline *a*-, *b*-, *c*-axes, and amorphous orientation functions for polyethylene. The uniaxial orientation is generally described by the Herman's factor:

$$f = \frac{3(\cos^2 \theta) - 1}{2} \quad (6)$$

where θ is the angle between the chain axis and the chosen reference axis (usually the machine direction). Most samples have a certain degree of symmetry with three orthogonal directions designated

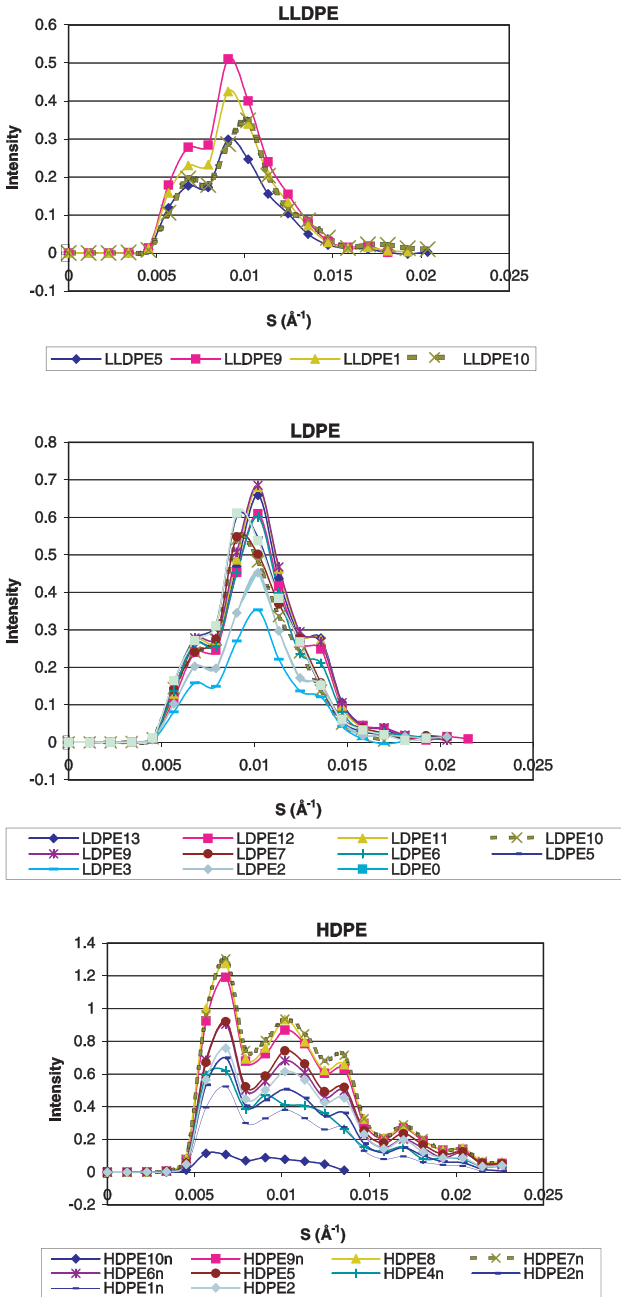


Figure 6. SAXS intensity distribution curves for LLDPE, LDPE, and HDPE films.

as machine (M), transverse (T), and normal (N). For polyethylene, the orientation functions for the a, b, and c crystallographic axis are defined as:

$$f_a = \frac{3 \cos^2 \alpha - 1}{2} \quad (7)$$

$$f_b = \frac{3 \cos^2 \beta - 1}{2} \quad (8)$$

$$f_c = \frac{3 \cos^2 \gamma - 1}{2} \quad (9)$$

where α , β , γ are the angles between the unit whose orientation is of interest (a-axis, b-axis, or c-axis) and a reference axis (M, T, or N). The three crystallographic axes are perpendicular such that:

$$f_a + f_b + f_c = 0 \quad (10)$$

A Nicolet 170SXFTIR (Magna-IR 860) was used to obtain the raw spectra at a resolution of 2 cm^{-1} with an accumulation of 128 scans using both a normal and tilted incidence. A deconvolution procedure was then applied in the $720\text{--}730 \text{ cm}^{-1}$ spectral region to determine the dichroic ratios and orientation functions [17,18].

The Herman's orientation functions were calculated using both the Pearson VII and Lorentzian equations in HDPE/LDPE samples, and Pearson in LLDPE samples at the region between 690 and 760 cm^{-1} [19,20]. This band could be decomposed by peak deconvolution techniques into three peaks. Two narrow peaks at 730 and 720 cm^{-1} arise from crystalline structure and a broader peak at 723 cm^{-1} arises from the amorphous phase.

Differential Scanning Calorimetry

Thermal analysis was performed using a Perkin-Elmer Pyris-7. The percentage of crystallinity of samples were obtained from DSC results and used as independent variables in the modeling. The heat of fusion of 100% crystalline PE was taken as 289 J/g [21] and the heating rate used was 10°C/min .

Birefringence

Birefringence is a measure of the total molecular orientation of a system. It is defined as the difference between the different refractive

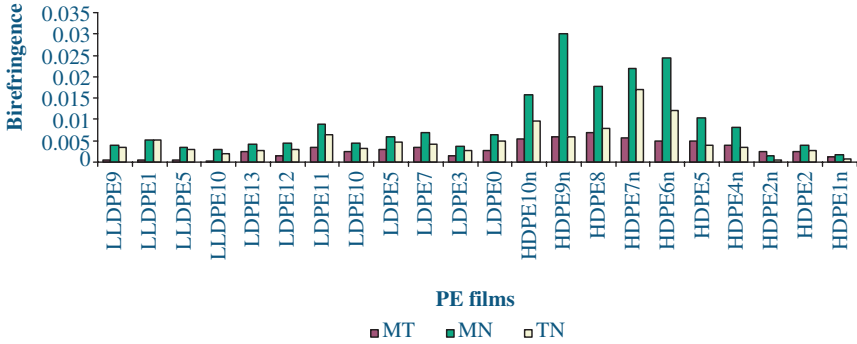


Figure 7. Birefringence in MD, TD, ND.

indices for the machine, transverse, and normal direction. $\Delta n_{MT} = n_M - n_T$, $\Delta n_{MN} = n_M - n_N$ and $\Delta n_{TN} = n_T - n_N$. The technique we use for its measurement is the multiwavelength polarized white light technique and light is directed through at least two beams at different angles. Figure 7 shows the results for birefringence in M, T, and N directions. It is obvious that HDPE films have a higher birefringence than that of LDPE and LLDPE films, which is due to the increase of the orientation caused by an increase in the TUR during production of HDPE films.

RESULTS AND DISCUSSION

Orientation Measurement

The orientation in both crystalline and amorphous phases is important in determining the mechanical properties of PE blown films. SEM was used to observe the orientation of lamellae and lamellar stacks directly. Further, the WAXD pole figure technique was used to obtain quantitative information about crystal orientation. Fourier transform infrared (FTIR) dichroism experiments were performed to compare with the WAXD results. The calculated Herman’s functions for crystalline a-, b-, c-axes and amorphous phase are shown in Figure 8. It is obvious from Figure 8(a) that the orientation function obtained from FTIR had quite a similar trend for all samples when compared with WAXD results, but the values from IR were higher than those from the WAXD pole figure technique. The amorphous orientation functions from FTIR technique were not reasonable (Figures 8(e), (f)), because the amorphous orientation should be more oriented in MD. In this work, the Herman’s factors that were obtained from the WAXD pole figure

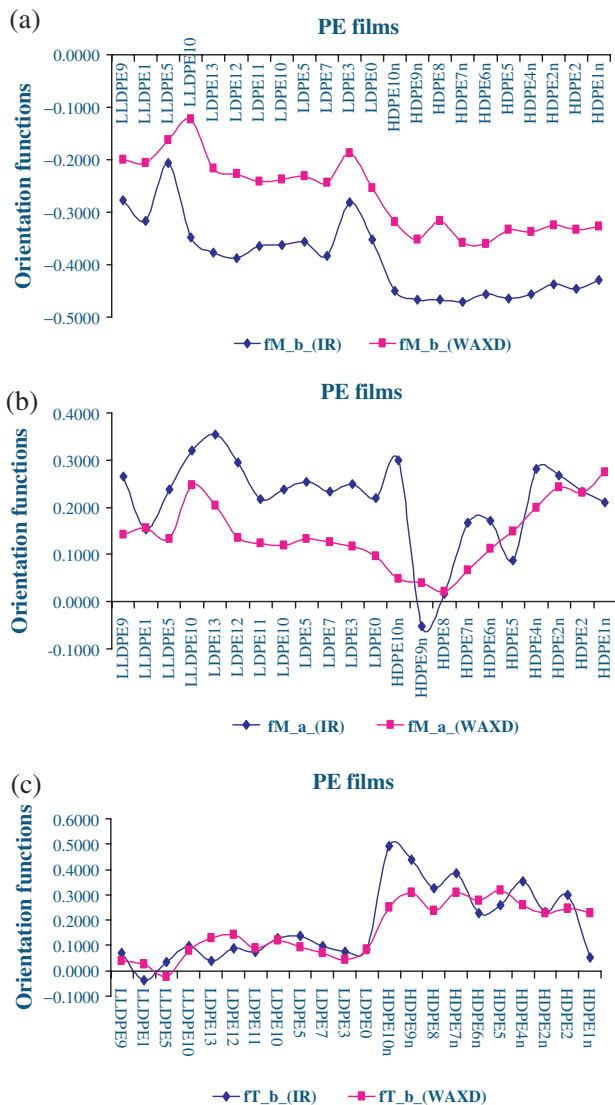


Figure 8. Measured orientation functions from two FTIR and WAXD techniques: (a) orientation factors of crystalline b-axis in MD; (b) orientation factors of crystalline a-axis in MD; (c) orientation factors of crystalline b-axis in TD; (d) orientation factors of crystalline a-axis in TD; (e) orientation factors of amorphous phase in MD; and (f) orientation factors of amorphous phase in TD.

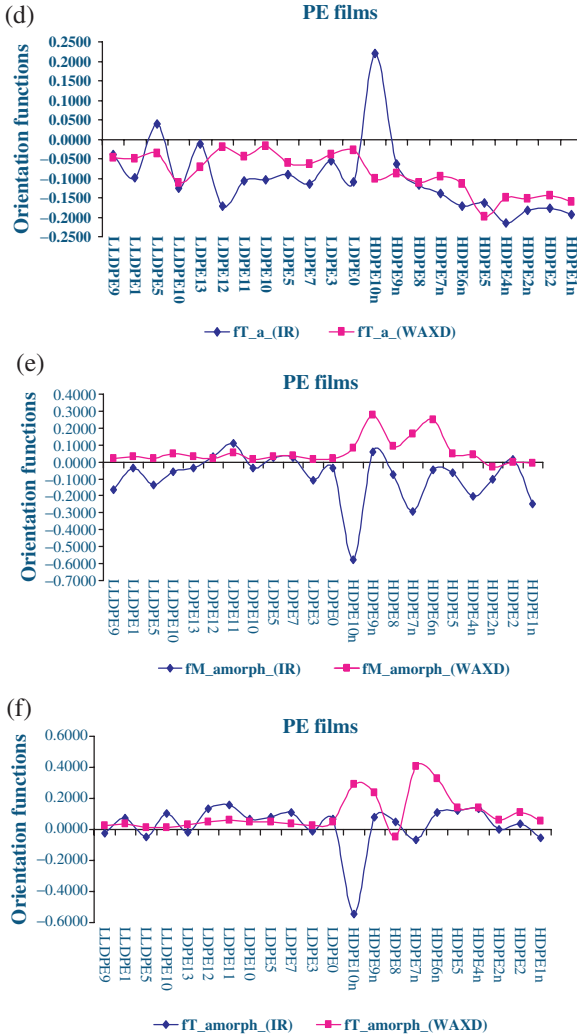


Figure 8. Continued.

technique were considered in statistical data analysis and the amorphous orientation functions were calculated from:

$$\Delta n = X_c f_c \Delta n_c^\circ + (1 - X_c) f_{am} \Delta n_{am}^\circ + \Delta n_{form} \quad (11)$$

where Δn is the birefringence of the polymer, f_c and f_{am} are the crystalline and amorphous orientation functions, Δn_c° and Δn_{am}°

are the intrinsic birefringence values for the perfectly oriented crystalline and amorphous phases, X_c is the crystal weight fraction, and Δn_{form} is the form birefringence due to the distortion of the electric field of the light wave at the anisotropic phase boundary. Δn_{form} is generally neglected, since it is just 5–10% of the total birefringence [22]. In the case of polyethylene, the value $\Delta n_c^\circ = 0.058$ was determined; $\Delta n_{\text{am}}^\circ$ values were found at various sources in the literature.

The crystalline contents were obtained by DSC and WAXD techniques and they were used in Equation (11) to calculate the amorphous orientation factors for MD and TD. The results are shown in Figure 9.

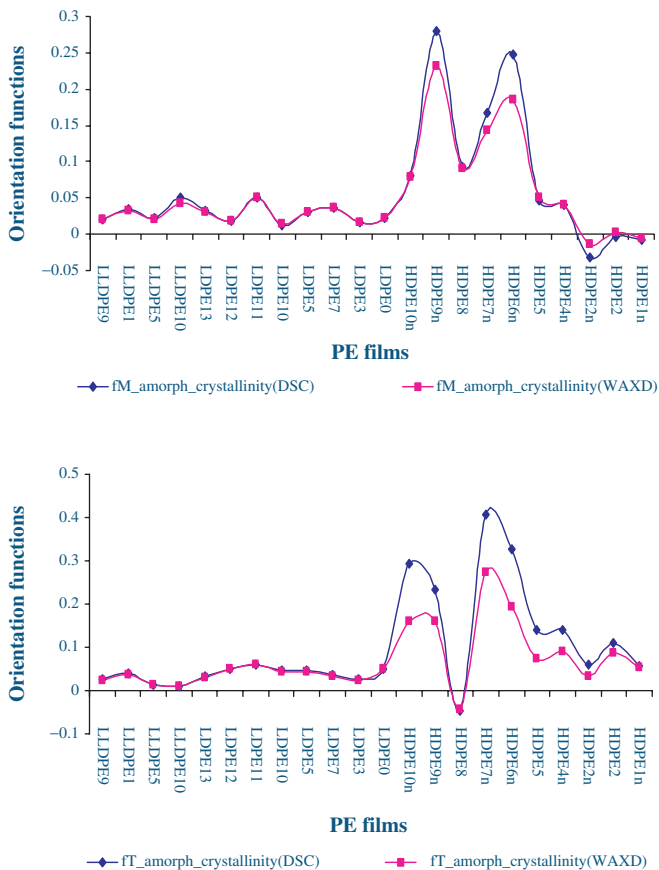


Figure 9. Amorphous orientation functions obtained using crystallinity from DSC and WAXD techniques.

Crystal Size and Lamellar Thickness Measurement

Lamellar thickness and its distribution are important morphological characteristics of semicrystalline polymers. The measurements of the dimensions of crystal and lamellar thickness were accomplished by SAXS, WAXD, and DSC techniques, because the melting temperature of polymer crystals is related to lamellar thickness.

The Gibbs–Thomson equation (simplified) and Wunderlich equation applied to obtain the thickness of lamellae at melt temperature [21,23].

$$l = \frac{2\sigma_e T_f^\circ}{\Delta H^\circ \rho_c (T_f^\circ - T_f)} \tag{12}$$

$$l = \frac{414.2 \times 0.627}{414.2 - T_f} \tag{13}$$

T_f and l are respectively the melt temperature (°K) and the thickness of lamellae, and σ_e is the basal surface free energy (one of the hypotheses is that the amount of σ_e for all samples – including LDPE, LLDPE, and HDPE – are constant at 90 erg/cm²), $\Delta H^\circ = 289$ J/g (Heat of fusion of 100% crystalline), $\rho_c = 0.995$ g/cm³ (the density of the crystalline phase), $T_f^\circ = 418.7^\circ$ K (melt temperature of 100% crystalline).

Figures 9 and 10 show that in the HDPE case, the gap between the results (orientation factors and lamellar thickness) from different methods is bigger than LLDPE and LDPE cases.

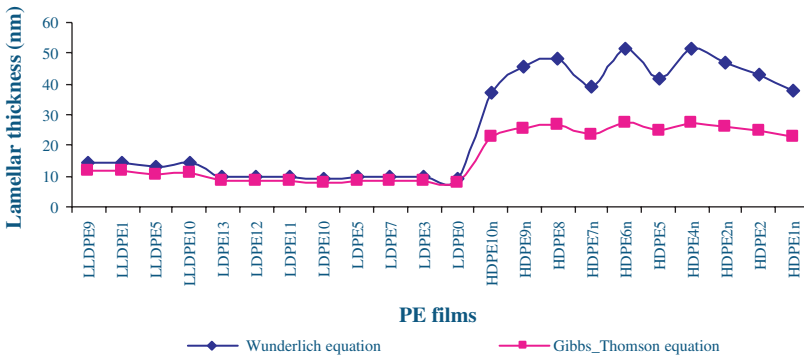


Figure 10. Measured lamellar thickness from two different equations.

Mechanical Property Measurements

The tensile properties of the films were evaluated according to ASTM D 882-02 using an Instron tensile testing machine at room temperature. The mechanical properties were measured in MD and TD directions for Young's modulus, elongation at break, elongation at yield, tensile strength at break, and tensile strength at yield. The tear strength (MD and TD tear resistance) of films was measured according to ASTM D1922. The haze was measured according to ASTM D 1003. The impact resistance of the films was evaluated in accordance with ASTM D1709-98. Some mechanical properties measured for the PE films are shown in Figure 11.

Design of Experiment

A statistical design of experiment was used to study the major effects between the micro-structural parameters and the properties of polyethylene films. The experiment consisted of 22 test runs (including 4 different samples for LLDPE, 8 samples for LDPE, 10 samples for HDPE) involving 12 independent variables. The independent variables and dependent variables (responses) are shown in Tables 3 and 4 respectively. These test data were used to generate equations to describe the factor effects on each of the mechanical and physical properties.

A stepwise regression approach was used and each response was regressed against all independent factors. The results of stepwise regression summary are shown in Table 5. Table 5 indicates which structure parameters caused a statistically significant (>95%) effect on the properties of the PE films. The parameters are listed down the left side of the table. The properties are listed across the top of the table. If a coefficient is listed on the line of a parameter, then that parameter has a significant effect on the corresponding property. These coefficients can be used to predict the individual film properties.

Based on the effects chart, it is obvious that there are correlations between the properties such as the modulus in MD and TD; tear strength in TD, tensile strength at break in MD and TD, tensile strength at yield in MD and TD, strain at break in MD and TD, strain at yield in MD and TD, haze and clarity with structural parameters including the crystalline content, lamellar thickness, orientation parameters for crystalline a-axis along MD, b-axis along MD and TD, the amorphous phase along MD and TD. For example, Table 5 shows that dart impact strength depends mainly on the lamellar thickness, crystal size (200), and orientation of the b-axis along MD and TD. The modulus in TD,

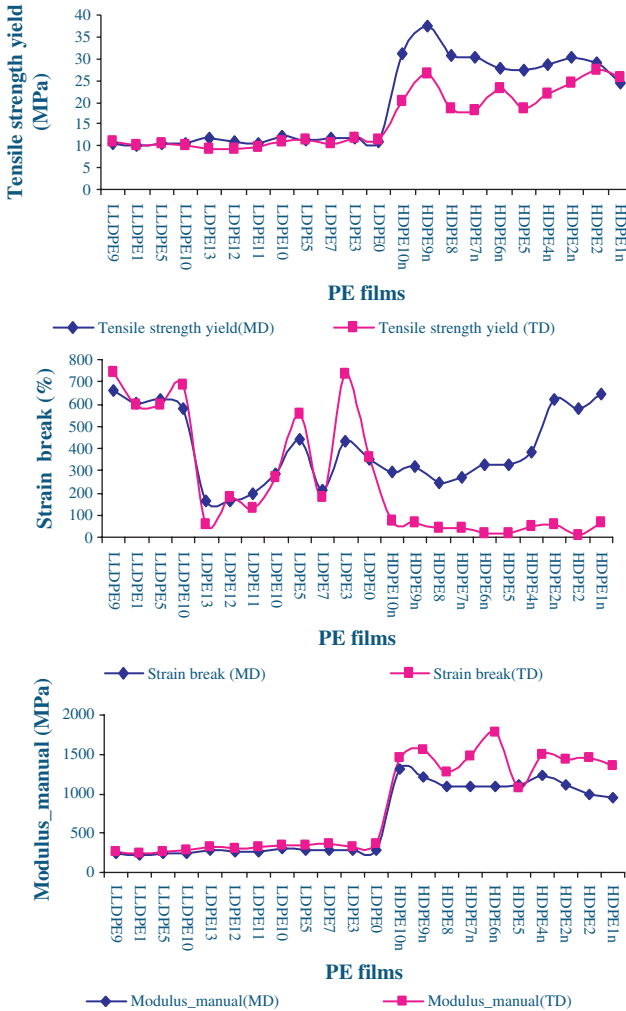


Figure 11. Measured mechanical properties.

the tensile strength at yield in MD and TD, haze and clarity are affected by the crystallinity.

From the statistical study concerning a set of independent values and a corresponding set of dependent values, it was found that some functional form will relate the dependent values to the independent values. The main approach in these studies was to select linear relationships as the functional form for the properties that show a

Table 3. Independent variables.

	Crystallinity	Crystal length (L_c)	Lamellar thickness	Crystal size (110)	Crystal size (200)	fM_a_ (WAXD)	fT_a_ (WAXD)	fM_b_ (WAXD)	fT_b_ (WAXD)	fM_amorph_ (WAXD)	fT_amorph_ (WAXD)	Roughness
LLDPE9	37.8	3.77	14.2	36.6	30.6	0.141	-0.048	-0.200	0.037	0.021	0.025	21.4
LLDPE1	41.4	4.16	14.6	36.2	30.4	0.155	-0.051	-0.206	0.025	0.034	0.039	11.7
LLDPE5	38.3	3.98	12.8	36.8	31.1	0.132	-0.036	-0.162	-0.025	0.022	0.013	31.5
LLDPE10	40.7	3.63	14.0	39.8	32.7	0.247	-0.111	-0.123	0.081	0.050	0.011	15.9
LDPE13	39.9	3.55	9.7	40.2	31.7	0.204	-0.073	-0.216	0.128	0.032	0.032	22.1
LDPE12	39.9	3.60	9.6	34.3	30.4	0.136	-0.020	-0.227	0.143	0.019	0.049	10.9
LDPE11	39.1	3.48	9.6	37.4	32.8	0.124	-0.045	-0.241	0.091	0.051	0.060	49.5
LDPE10	42.2	4.24	8.9	36.5	32.8	0.120	-0.018	-0.237	0.118	0.013	0.048	28.2
LDPE7	41.2	4.14	9.6	40.7	33.7	0.126	-0.064	-0.243	0.069	0.036	0.037	8.4
LDPE5	41.2	4.14	9.6	39.6	31.5	0.133	-0.060	-0.232	0.094	0.030	0.046	13.5
LDPE3	42.1	3.76	9.6	36.0	32.9	0.116	-0.038	-0.187	0.045	0.017	0.026	19.2
LDPE0	37.7	4.18	9.4	36.1	32.0	0.097	-0.028	-0.255	0.086	0.023	0.049	14.4
HDPE10n	72.6	12.25	37.0	49.7	37.9	0.049	-0.100	-0.318	0.252	0.080	0.292	33.6
HDPE9n	68.6	9.59	45.7	46.8	36.4	0.040	-0.089	-0.353	0.308	0.279	0.235	28.0
HDPE8	70.2	9.84	48.5	47.2	38.0	-0.024	-0.112	-0.317	0.303	0.094	-0.048	67.2
HDPE7n	68.7	9.61	38.9	46.5	35.9	0.066	-0.097	-0.357	0.309	0.167	0.407	46.8
HDPE6n	71.3	10.01	51.8	51.0	41.1	0.113	-0.116	-0.361	0.277	0.248	0.327	69.4
HDPE5	69.3	9.69	42.0	47.0	38.2	0.148	-0.199	-0.334	0.315	0.047	0.141	23.6
HDPE4n	71.8	10.08	51.8	40.7	36.9	0.198	-0.150	-0.338	0.258	0.041	0.141	24.6
HDPE2n	70.7	9.91	47.1	48.7	39.6	0.243	-0.154	-0.326	0.227	-0.032	0.058	54.5
HDPE2	69.5	9.73	43.2	46.7	35.3	0.232	-0.145	-0.334	0.246	-0.003	0.109	21.3
HDPE1n	69.7	9.76	37.9	43.9	33.5	0.274	-0.160	-0.326	0.228	-0.007	0.057	62.1

Table 4. Dependent variables.

	MD		MD		MD modulus		TD		TD		TD modulus		DART impact	Tear strength		Haze (%)	Clarity (%)
	tensile strength yield (MPa)	strain at yield (%)	tensile strength break (MPa)	strain break (%)	Manual	Automatic	tensile strength yield (MPa)	strain at yield (%)	tensile strength break (MPa)	strain at break (%)	Manual	Automatic		(g)	MD (g/μm)		
LLDPE9	10.5	14.0	31.9	660	236	232	10.9	13.7	29.4	747	261	256	296.0	16.1	28.2	9.7	98.8
LLDPE1	10.1	13.4	30.0	601	223	218	10.1	12.6	18.2	597	246	247	336.0	14.8	27.2	6.4	97.9
LLDPE5	10.5	13.3	23.4	622	234	234	10.5	14.1	17.9	593	264	259	480.0	17.3	24.2	8.2	99.0
LLDPE10	10.5	12.0	38.5	576	241	227	10.3	10.7	20.8	687	277	278	174.0	8.9	29.6	5.2	99.0
LDPE13	11.9	12.1	14.5	165	287	222	9.1	4.6	4.9	61	329	327	15.8	7.3	8.2	6.3	91.2
LDPE12	11.0	11.9	16.3	166	260	201	9.2	6.4	5.4	177	313	312	4.0	9.4	7.4	6.0	92.0
LDPE11	10.7	12.4	14.2	197	256	194	9.8	6.8	5.0	132	324	326	6.8	7.2	8.9	6.5	90.3
LDPE10	12.1	11.9	10.1	283	298	251	10.8	8.1	7.6	266	349	347	11.8	9.6	12.1	6.4	91.9
LDPE7	11.7	12.6	12.8	210	290	224	10.6	7.9	5.2	176	362	362	13.9	12.3	9.5	7.0	91.0
LDPE5	11.2	13.2	16.4	442	274	222	11.2	9.3	11.1	552	348	347	22.3	28.3	21.6	6.4	93.7
LDPE3	11.6	14.6	10.3	432	289	284	11.9	11.8	14.6	738	333	326	49.5	4.9	8.1	9.4	92.4
LDPE0	10.9	14.1	12.3	354	280	217	11.3	9.3	8.7	361	354	354	38.5	8.7	10.8	9.6	86.4
HDPE10n	31.1	4.8	58.3	293	1304	1186	20.4	2.2	14.9	71	1445	1520	0.0	0.6	7.9	54.5	34.9
HDPE9n	37.5	6.0	71.4	318	1222	1113	26.4	3.2	17.1	65	1554	1372	0.0	0.2	12.2	51.3	34.7
HDPE8	30.9	6.0	44.2	244	1095	933	18.6	2.3	12.2	37	1275	1279	0.0	0.3	9.3	58.1	33.0
HDPE7n	30.2	5.3	46.7	273	1099	1048	18.3	2.0	8.8	42	1481	1537	0.0	0.3	16.1	58.4	32.5
HDPE6n	27.8	4.7	38.5	325	1086	1113	23.0	1.6	16.4	13	1783	1800	0.0	0.4	16.0	63.3	26.0
HDPE5	27.4	5.0	35.1	327	1109	1096	18.6	2.7	12.2	16	1075	1090	0.0	0.2	13.1	71.3	19.5
HDPE4n	28.5	4.5	46.8	383	1226	1230	22.0	2.4	12.0	48	1489	1499	0.0	0.3	29.6	65.2	24.9
HDPE2n	30.2	6.5	44.2	622	1113	1108	24.4	2.4	16.8	54	1441	1461	1.3	0.5	38.3	74.4	16.0
HDPE2	29.1	6.7	47.5	583	988	1009	27.5	2.6	21.4	7	1453	1468	3.8	0.2	24.3	70.6	17.8
HDPE1n	24.6	6.5	31.3	645	954	1015	25.7	2.8	16.4	68	1356	1363	3.7	0.4	17.8	72.9	15.6

linear relationship. A linear equation or mathematical model explicitly defining the dependent variables (properties) is obtained of the form:

$$\text{Property} = A + B(X_1) + C(X_2) + \dots$$

where B, C, ... are regression coefficients and A is a pure constant. X_1, X_2, \dots are the independent variables. For example, Modulus TD (AUT) can be calculated by this equation using Table 5:

$$\begin{aligned} \text{Modulus (TD)} = & (A + 0.61 \times \text{Crystallinity}) + (0.3 \times \text{lamellar thickness}) \\ & + (0.15 \times f M_a) + (0.26 \times f T_a) + (0.11 \times f T_{\text{amorph}}) \end{aligned}$$

From Tables 3 and 4, it is obvious that the information gained through the statistical study can be used to determine the effects of parameters on each property, but it should be pointed out that the statistical approach was based on a limited set of experiments (22 test runs) and thus are not definitive. For example, in the case of dependency of tensile strength break at MD on roughness and the independence of Dart impact strength on crystallinity, there is no explanation. Although it is generally accepted that the effects chart could provide guidance to develop practical, predictive models for the estimation of PE film properties, it is clear that it requires more test runs at commercial production levels to determine the desired factor effects that are under study.

CONCLUSION

A systematic investigation provided fundamental understanding on the interrelations between polyethylene films' structural parameters (crystallinity, crystallite dimensions, and arrangement, orientation etc.) and physical properties. Different techniques for characterizing the film structure included birefringence, WAXD, SAXS and AFM, X-ray pole figure analysis, SEM, and infrared radiation. These techniques were used for determination and calculation of structural parameters and the morphology of the films.

By changing the processing conditions and producing different structures for LDPE, LLDPE, and HDPE blown films, the study of the above structural parameters was combined with measuring the physical and mechanical properties (tensile properties, tear strength,

dart impact strength, haze and clarity), so that models for each property were defined.

Statistical analysis showed that parameters such as lamellar thickness, crystallinity and orientation factors have a significant effect on most film properties. Tear strength, dart impact strength, tensile and optical properties are important in many film applications; and based on the statistical technique it was observed that many of these properties correlate with various structure parameters (crystalline content, orientation functions for crystalline a-axis along MD and TD, b-axis along MD and TD, amorphous along MD and TD, lamellar thickness, and roughness).

REFERENCES

1. Lu, J., Zhao, B. and Sue, H.-J. (1999). *ANTEC Proceedings*, pp. 1768–1774.
2. Krishnaswamy, R.K. and Sukhadia, A.M. (2000). *Polymer*, **41**(26): 9205–9217.
3. Krishnaswamy, R.K. (2001). Structure-property Relationships in HMW-HDPE Blown Films, In: *ANTEC Proceedings*, pp. 111–115.
4. Babel, A.K., Nagarajan, G. and Campbell, G.A. (1996). *ANTEC Proceedings*, pp. 2112–2119.
5. Lu, J. and Sue, H.-J. (2000). *J. Materials Sci.*, **35**(20): 5169–5178.
6. Patel, R.M., Butler, T.I., Walton, K.L. and Knight, G.W. (1994). *Polymer Engineering and Science*, **34**(19): 1506–1514.
7. Simpson, D.M. and Harrison, I.R. (1993). *ANTEC Proceedings*, pp. 1206–1209; also (1994). A Study of the Effects of Processing Parameters on the Morphologies and Tensile Modulus of HDPE Blown Films: Application of Composite Theories on a Molecular Level to Characterize Tensile Modulus, *J. Plas. Film & Sheeting*, **10**(4): 302–325.
8. Kim, Y.-M., Kim, C.-H., Park, J.-K., Lee, C.-W. and Min, T.-I. (1997). *J. Appl. Polym. Sci.*, **63**(3): 289–299.
9. Sukhadia, A.M. (1998). *ANTEC Proceedings*, pp. 160–168.
10. Godshall, D., Wilkes, G., Krishnaswamy, R.K. and Sukhadia, A.M. (2003). *Polymer*, **44**(18): 5397–5406.
11. Haudin, M.J., Piana, A., Monasse, B. and Gourdon, B. (2003). *Ann. Chim. Sci. Mat.*, **28**(1): 91–107.
12. Krishnaswamy, R.K. and Sukhadia, A.M. (2002). *ANTEC Proceedings*, pp. 2395–2399; also (2005). The Influence of Solid-state Morphology on the Dart Impact Strength of LLDPE Blown Films, *J. Plas. Film & Sheeting*, **21**(2): 145–158.
13. Aji, A. and Zhang, X. (2002). *ANTEC Proceedings*, pp. 1651–1655.

14. Lu, J. and Sue, H. (2002). *J. Polymer Sci. (Physics Edition)*, **40**(6): 507–518.
15. Ghaneh-Fard, A. (1999). Effects of Film Blowing Conditions on Molecular Orientation and Mechanical Properties of PE Films, *J. Plas. Film & Sheeting*, **15**(3): 194–218.
16. Chai, K.C., Selo, J.-L. and Osmont, E. (2000). Influence of Molecular Weight Distribution on LLDPE Blown Film Processing Conditions and Property Sensitivity, In: *ANTEC Proceedings*, pp. 331–335.
17. Zhang, X.M., Verilhac, J.M. and Ajji, A. (2001). *Polymer*, **42**(19): 8179–8195.
18. Cole, K.C. and Ajji, A. (2000). In: Ward, I.M., Coates, P.D. and Dumoulin, M.M. (eds), *Characterization of Orientation in Solid Phase Processing of Polymers*, Carl Hanser Verlag, Munich.
19. Heuvel, H.M. and Huisman, R. (1985). *J. Appl. Polym. Sci.*, **30**(7): 3069–3093.
20. Cole, K.C., Legros, N. and Ajji, A. (1998). *SPE Conference Proceedings on Orientation of Polymers*, pp. 322–334.
21. Hoffman, D.J. and Miller, L.R. (1997). *Polymer*, **38**(13): 3151–3212.
22. Stein, R.S. (1963). *Newer Methods in Polymer Characterization*, Chap. IV, Wiley-Interscience, New York.
23. Hohné, G.W.H. (2002). Another Approach to the Gibbs-Thomson Equation and the Melting Point of Polymers and Oligomers, *Polymer*, **43**(17): 4689–4698.

BIOGRAPHIES

Shokoh Fatahi

Shokoh Fatahi obtained her BScA in Chemical Engineering from Tehran Polytechnique (Iran) and MScA in Polymer Engineering from Tehran University. She worked in Sanandaj University for one year before joining National Petrochemical Industries Company of Iran for 12 years as a Senior Process Engineer of polyolefin plants. She is the author of two books: ‘Piping Calculation in Fluid Flow’ and ‘Petroleum Resins’. She is currently a PhD student in the Chemical Engineering department of École Polytechnique de Montreal where her project is about correlation between different micro-structure parameters with physical/mechanical properties of polyethylene blown films.

Pierre G. Lafleur

Pierre Lafleur obtained his BScA and MScA in Chemical Engineering from École Polytechnique de Montreal and a PhD in Chemical Engineering (polymer processing) at McGill University. He is currently

the Professor of Chemical Engineering and the Dean of Studies at École Polytechnique de Montreal. He has been active in research for over 25 years in the field of single and twin screw extrusion and the film blowing process. He has published over 75 articles in peer-reviewed scientific journals.

Abdellah Aji

Abdellah Aji earned his MScA and PhD in Chemical Engineering from École Polytechnique de Montreal and worked in research and development on polymers – particularly orientation of polymer films, rheology and blends – for the past 19 years. He is currently a Senior Research Officer at the Industrial Materials Institute of the National Research Council of Canada and has over 75 published articles in scientific journals.